

# DESIGN OF A NEW SUPERCONDUCTING LINAC FOR THE RIBF UPGRADE

K. Yamada\*, K. Suda, N. Sakamoto, O. Kamigaito,  
RIKEN Nishina Center, Wako, Saitama 351-0198, Japan

## Abstract

An upgrade plan for the RIKEN Radioactive Isotope Beam Factory is under discussion, the objective being to significantly increase the uranium beam intensity. In the upgrade plan, the existing RIKEN ring cyclotron (RRC) will be replaced by a new linac, mainly consisting of superconducting (SC) cavities. The new linac is designed to accelerate heavy ions with a mass-to-charge ratio of  $\sim 7$  (e.g.,  $^{238}\text{U}^{35+}$ ) up to an energy of 11 MeV/u in the cw mode. A conceptual design of the SC section was devised based on a first-order approximation for the transverse and longitudinal motions. The rf design of the SC cavity was tested using CST Microwave Studio. Further study on the SC cavity, including mechanical considerations, is underway using ANSYS. We also report a preliminary design of the cryostat.

## INTRODUCTION

The beam intensity of the Radioactive Isotope Beam Factory (RIBF) [1] at the RIKEN Nishina Center has been rapidly increased owing to continuous efforts in the past few years [2, 3]. Among its various heavy-ion beams, the uranium beam is one of the most important, because the in-flight fission of uranium ions can produce intense neutron-rich radioactive isotope (RI) beams far from the stability line on the nuclear chart. The maximum intensity of the uranium beam has recently reached 25 pA ( $\approx 10^{11}$  pps) at 345 MeV/u by introducing a new 28-GHz superconducting electron cyclotron resonance (ECR) ion source [4, 5], the new injector linac RILAC2 [6, 7], and a new charge stripping system [8,9] and by optimization of operational parameters. The intensity of the uranium beam is to be increased to  $>50$  pA in the next few years using the present acceleration system.

Recently, an upgrade plan for the RIBF has been proposed with the objective of expanding its capabilities to study nuclear reaction mechanisms with RI beams. The intensity of the uranium beam mentioned above is, however, insufficient to meet this demand; it should be at least an order of magnitude higher than the maximum achievable intensity with the present RIBF accelerators. The difficulty in the present acceleration scheme shown in the upper drawing of Fig. 1 mainly stems from the two-stage charge strippers located at 11 and 50 MeV/u, respectively, which yields a maximum total stripping efficiency of only 5%. In addition, the low acceleration voltage of the RIKEN ring cyclotron (RRC), which is about 280 kV/turn at an operating frequency of 18.25 MHz for uranium acceleration, causes beam losses at the extraction point of the RRC because of the significant influence of space-charge effects.

Therefore, we proposed the new acceleration scheme shown in the lower drawing of Fig. 1. In the upgrade plan, the fixed-frequency ring cyclotron (fRC) will be replaced by a new cyclotron [10] that will be designed to accept  $\text{U}^{35+}$  ions without charge stripping at 11 MeV/u, and the RILAC2+RRC will be replaced by a new linac injector, mainly consisting of superconducting (SC) cavities, to improve the transmission efficiency of the high-current beam. By making these modifications, we aim to increase the beam intensity by at least one order of magnitude compared to the achievable beam intensity with the present accelerator chain. To evaluate the feasibility of the new linac injector, we initiated a design study of the SC linac in fiscal year 2013 [11].

## OVERVIEW OF THE NEW LINAC INJECTOR

A layout plan of the new linac is shown in Fig. 2. Heavy ions with a mass-to-charge ratio ( $m/q$ ) of  $\sim 7$  (e.g.,  $^{238}\text{U}^{35+}$  and  $^{124}\text{Xe}^{19+}$ ) are designed to be accelerated up to 1.4 MeV/u by a short room-temperature (RT) section, and they are boosted up to 11 MeV/u with the succeeding SC section in the cw mode. The beam energy at the border of the RT and SC sections was chosen so that the SC section could be covered by a single structure of a quarter-wavelength resonator (QWR) with two acceleration gaps.

The rf of the SC-QWR was chosen to be 73 MHz, which is twice that of the RT section, and the gap voltage was assumed to be 800 kV. Because a broad range of velocities had to be covered, the gap length  $g$  and the length  $d$  between the gap centers of the SC-QWR were optimized to minimize the number of QWRs in the section [11]; we have determined the length as  $d = 160$  mm and a total cavity number of 56.

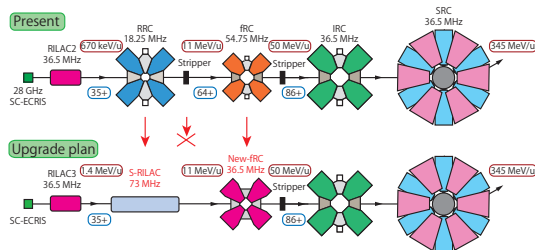


Figure 1: Present (upper drawing) and proposed (lower drawing) accelerator chains for the uranium beam at the RIBF. The final beam energy is 345 MeV/u. The radio frequencies, stripping energies, and charge states are indicated.

\* nari-yamada@riken.jp

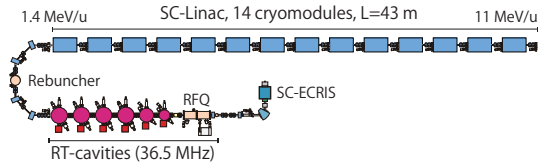


Figure 2: Layout plan of the new linac injector.

The gap length was also set to be  $g = 60$  mm. The value of  $d$  corresponds to  $\beta_{\text{geom}} = 0.078$  through the relation  $d = \beta_{\text{geom}} \lambda / 2$ . The modular configuration of the SC section was optimized based on a first-order approximation for the transverse and longitudinal motions [11]. Several configurations were checked to determine whether a semiperiodic envelope could be obtained with moderate-strength focusing elements, while keeping the longitudinal acceptance large enough to capture the output beam from the RT section. Finally, we chose a configuration that consists of 14 cryomodules, each of which contains four SC-QWRs, and a RT quadrupole doublet placed in each space between the cryomodules. This configuration did not give the best longitudinal acceptance among the configurations; however, the advantage is that the RT quadrupoles, having an aperture diameter of 50 mm and a field gradient of  $<20$  T/m, would be easier for us to make and operate compared to the SC solenoid. The total length will be 43 m for the SC section.

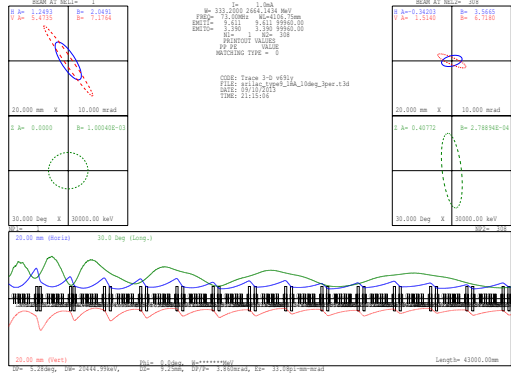


Figure 3: Transverse and longitudinal beam envelopes plotted by using the TRACE3-D code.

The transverse and longitudinal beam envelopes of the configuration are plotted by using the TRACE3-D code [12] in Fig. 3. The initial longitudinal ellipse was assumed to have a phase spread of  $\Delta\phi = \pm 10^\circ$  and an energy spread of  $\Delta E/E = \pm 3.0\%$ ; these values were larger than the calculated longitudinal emittance of the output beam from the RT section. As shown in Fig. 3, the envelopes are kept small enough.

## DESIGN STUDY OF COMPONENTS

### SC-QWR

After selecting the initial design of the SC-QWR described in Ref. [11], we optimized the shape of SC-QWR to reduce the rf power loss using CST Microwave Studio

(MWS). The left panel of Fig. 4 shows the magnetic-field distribution in the SC-QWR after the optimization. The rf power loss was reduced by about 20% compared with that of the initial design. The new design parameters are listed in Table 1; the definition of the effective length for the determination of  $E_{\text{acc}}$  is selected to be  $\beta_{\text{geom}} \lambda$ .

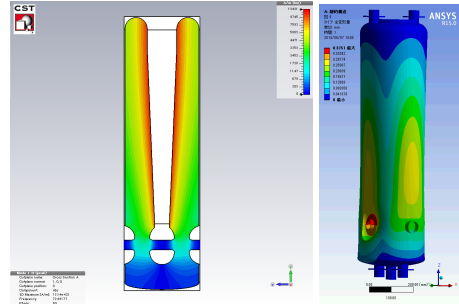


Figure 4: Magnetic-field strength of the SC-QWR calculated by using MWS (left) and deformation for the case of pressing the beam ports calculated by using ANSYS (right).

Table 1: Design Parameters of the SC-QWR of the New Linac

Frequency [MHz]	73
Duty [%]	100
Cavity inner diameter [mm]	$\phi 300$
Cavity height [mm]	1103
Gap length $g$ [mm]	60
Gap voltage $V_{\text{gap}}$ [kV]	800
$\beta_{\text{geom}}$ of cavity	0.078
Beam aperture $a$ [mm]	$\phi 40$
Synchronous phase $\phi_s$ for $\beta_{\text{geom}}$ [ $^\circ$ ]	$-25$
Operating temperature $T$ [K]	4.5
$G = Q_0 \times R_s$ [ $\Omega$ ]	22.6
$R_a/Q_0$ [ $\Omega$ ]	718
$R_s = R_{\text{BCS}} + R_{\text{res}}$ [n $\Omega$ ]	25
$Q_0$	$9.0 \times 10^8$
Shunt impedance $R_a$ [ $\Omega$ ]	$6.5 \times 10^{11}$
rf power loss $P$ [W]	4.0
$E_{\text{acc}}$ [MV/m]	4.5
$E_{\text{peak}}/E_{\text{acc}}$	6.0
$B_{\text{peak}}/E_{\text{acc}}$ [mT/(MV/m)]	9.5

To design the tuner system of the cavity, we investigated the mechanical deformation of the SC-QWR using ANSYS mechanical and CST MPHYSICS in parallel. In these first-step calculations, the helium jacket was omitted, and the thickness of the bulk niobium was assumed to be 4 mm. The calculations were performed by changing the pressing positions and the mechanical constraints on the cavity boundaries. The frequency variation resulting from the deformation was also calculated by using MWS for every condition. The right panel of Fig. 4 shows the result of the deformation calculated under the condition of pressing the beam ports by a load of 5000 N with the perpendicular side being free.

The resultant values for the condition are as follows: The maximum deformation is  $\sim 0.38$  mm, the maximum stress is  $\sim 120$  MPa, and the frequency variation is  $-9.40$  kHz, which corresponds to a sensitivity of  $-24.75$  kHz/mm. According to these result, sufficient deformation and frequency tuning range can be obtained by pressing the beam ports, although the maximum stress greatly exceeds the tolerable limit. Because a reduction of the pressing force by one order of magnitude is required to realize a reasonable tuner system, we are going to investigate a more suitable structure around the joint of the end drift tube.

### Beam Steering Effect

Because of the asymmetry of the QWR structure, the beam is steered by the rf magnetic field accumulatively downward at the acceleration gaps. Ostroumov and Shepard [13] suggest a serious emittance growth in the low-velocity region by the beam steering effect. To investigate the influence of this effect, the beam trajectory was simulated by a Runge-Kutta-Gill method based on the calculated field data by using the MWS code, and the magnetic-field distribution was deduced from the electric-field data. The space-charge effect was not taken into account.

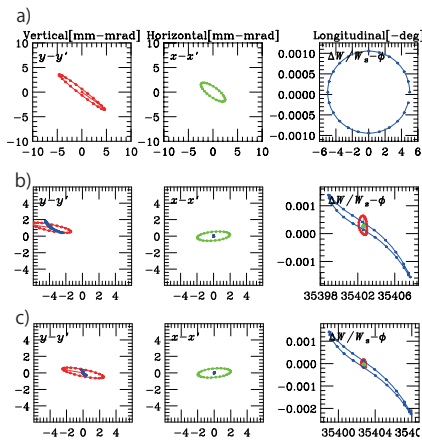


Figure 5: Input (a) and exit (b, c) beam ellipses. The corrections by steering magnets are included in (c).

It was found that, for the  $^{238}\text{U}^{35+}$  beam, the central beam particle was deflected  $\sim 1.8$  mrad downward in the first cryomodule, and the trajectory was shifted  $\sim 1.8$  mm at the exit of the cryomodule. Figure 5(a) shows the input beam ellipse, and Fig. 5(b) indicates the beam ellipse at the exit calculated for the whole of the SC section. As shown in Fig. 5(b), the overall shift of the beam centroid is  $\sim -4$  mm, and the longitudinal emittance is affected by the vertical motion. By correcting the beam shift in every cryomodule with steering magnets placed in each gap between the cryomodules, the emittance coupling can be well controlled, as shown in Fig. 5(c). Owing to the use of quadrupole magnets, the emittance growth caused by the beam steering effect seems to be negligible. However, the steering compensation should be done very carefully because the adjustment of the steering magnets changes the beam energy and causes

a variation of the bunching phase at the injection of the succeeding cyclotron. Thus, we are going to optimize the edge angle of the drift tubes, as shown in Ref. [13], to minimize the steering effect. Further investigation is also required for the simulation by taking space-charge effects into account.

### Cryostat

This fiscal year we began developing the conceptual design of the cryostat. The required components such as valves and pipes were investigated and the assembly procedure was verified. Figure 6 shows the first design of the cryostat assembly. We adopted a separate valve box for the liquid-helium cooling system. The rf input couplers will be inserted into the SC-QWR through the bottom ports. A magnetic shield will surround the inner equipment as a whole.

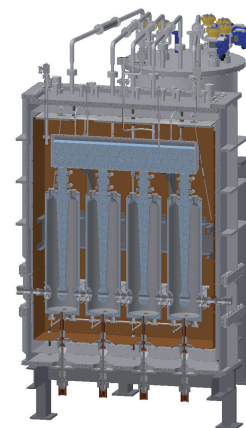


Figure 6: First conceptual design of a cryostat assembly.

## OUTLOOK

We have obtained a reasonable solution to meet the requirements of the new linac injector for the RIBF. Further study is underway on the SC-QWR, including mechanical considerations, tuner design, and coupler design. In parallel, we are going to begin thermal and mechanical studies of cryostats based on the initial design shown above. We plan to fabricate a bulk niobium cavity for testing in the near future.

## REFERENCES

- [1] Y. Yano, Nucl. Instrum. Methods B **261** (2007) 1009.
- [2] H. Okuno, N. Fukunishi, O. Kamigaito, Prog. Theor. Exp. Phys. (2012) 03C002.
- [3] N. Fukunishi et al., Proc. Cyclotrons 2013, MO1PB01 (2013).
- [4] T. Nakagawa et al., Rev. Sci. Instrum. **81** (2010) 02A320.
- [5] Y. Higurashi et al., Rev. Sci. Instrum. **83** (2012) 02A308.
- [6] K. Yamada et al., Proc. IPAC 2012, TUOBA02, (2012) 1071.
- [7] K. Suda et al., Nucl. Instrum. Methods A **722** (2013) 55.

- [8] H. Imao et al., Phys. Rev. Spec. Top.–Accel. Beams **15** (2012) 123501.
- [9] H. Hasebe et al., RIKEN Accel. Prog. Rep. **46** (2013) 133.
- [10] J. Ohnishi et al., Proc. Cyclotrons 2013, MOPPT022 (2013).
- [11] K. Yamada et al., Proc. SRF 2013, MOP021, (2014) 137.
- [12] [http://laacg.lanl.gov/laacg/services/download\\_trace.phtml](http://laacg.lanl.gov/laacg/services/download_trace.phtml).
- [13] P.N. Ostroumov and K.W. Shepard, Phys. Rev. Spec. Top.–Accel. Beams **4** (2001) 110101.